Received March 21, 2019, accepted April 4, 2019, date of publication April 9, 2019, date of current version April 18, 2019.

Digital Object Identifier 10.1109/ACCESS.2019.2909810

A Reconfigurable MIMO/UWB MIMO Antenna for Cognitive Radio Applications

XIONGWEN ZHAO, (Senior Member, IEEE), SHARJEEL RIAZ, AND SUIYAN GENG
School of Electrical and Electronic Engineering, North China Electric Power University, Beijing 102206, China

Corresponding author: Sharjeel Riaz (sharjeelrz@gmail.com)

This work was supported in part by the Key program of Beijing Municipal Natural Science Foundation under Grant 17L20052, in part by the Beijing Municipal Science and Technology Commission under Grant Z181100003218007, and in part by the National Nature Science Foundation of China (NSFC) under Grant 61771194.

ABSTRACT A novel multi-mode frequency reconfigurable MIMO and an ultrawideband (UWB) MIMO antenna design for cognitive radio applications is proposed in this paper. The antenna structure contains two modified triangular-shaped printed monopole antenna elements and a combination of varactor and PIN diodes. The proposed antenna has three operating modes: UWB mode for spectrum sensing, a frequency reconfigurable MIMO mode for communication over different frequencies, and UWB antenna operating in MIMO configuration. The UWB mode and reconfigurable communication mode are obtained by utilizing different switching ON/OFF states of PIN and varactor diodes. In the UWB mode, the antenna can cover the spectrum from 1 to 4.5 GHz, while it achieves the frequency reconfigurability over a wide range from 0.9 to 2.6 GHz using varactor diode tuning in the reconfigurable communication mode. The proposed antenna has a compact and planar structure with overall dimensions of $120 \times 60 \times 1.5$ mm^3. The proposed design also exhibits good MIMO performance; the minimum isolation measured is 12.5 dB, while the envelope correlation coefficient (ECC) of less than 0.19 is achieved for the whole operating band. To validate the proposed concept, the prototype of the antenna system is fabricated and measured. The simulation results are in good agreement with the measurement results.

INDEX TERMS Cognitive radio (CR), frequency reconfigurable antenna, MIMO, PIN diodes, ultrawideband (UWB), varactor diode.

I. INTRODUCTION

Cognitive radio (CR) has appeared as a revolutionary technology for dynamic, efficient and flexible utilization of the scarce frequency spectrum [1]. A CR system architecture includes two antennas: ultrawideband (UWB) sensing antenna for constant monitoring of the unoccupied frequency channels and a reconfigurable communication antenna for communication within those unoccupied channels [2]. Majority of designs reported in literature for CR applications employ separate antennas for spectrum sensing and communication purposes. However, the use of two different antennas results in large physical size, more space requirement and complex structure, which is not suitable for today's communication. Thus, to deal with these limitations, a single antenna capable of both communicating and sensing is very desirable for cognitive radio communication.

The associate editor coordinating the review of this manuscript and approving it for publication was Chan Hwang See.

In CR system, they are two user types i.e. primary users (PUs) which are licensed users and the secondary users (SUs) who are unlicensed users. SUs can access the channel when PUs are inactive. PUs have no restrictions on their transmitted power whereas SUs must transmit without producing any interference with already present PUs. Generally, there can be two methods for spectrum sharing in CR: interweave spectrum sharing and underlay spectrum sharing. For the spectrum interweave CR, the SUs transmit only at idle frequencies. In underlay case, SUs always transmit the signal inside the tolerable interference level set by PUs. The PUs and SUs can share the same channel. This is allowable only if the PUs can sustain the interference caused by SUs. This work presents an underlay antenna system where quality of service for PUs is not affected as SUs only transmit within the allowable interference levels.

A smart antenna having CR compatibility and compact size is an essential requirement for modern wireless communication systems. Therefore, several antenna designs for

CR systems can be found in literature [3]–[15]. Antenna designs that incorporated both the communication reconfigurable antenna and the UWB sensing antenna into the same substrate were presented in [3]–[9]. In [3], a five-element UWB and narrowband integrated antenna system was presented. The UWB antenna had sensing capability from 3.1 to 10.6 GHz while four narrowband antennas had four operating bands: 8.7-9.92 GHz, 9.82-10.74 GHz, 3.06-4.23 GHz and 6.33-8.83 GHz. In [4], the UWB antenna can operate between 2-12 GHz while reconfigurable structure use PIN diodes to operate at six different frequency bands: 5.65 GHz, 5 GHz, 3.6 GHz, 2.94 GHz, 2.15 GHz, 4.5 GHz and two dual-bands at 2 and 5.48 GHz, 1.7 and 5 GHz. In [5], varactor diode was used to achieve frequency reconfigurability from 5 to 6 GHz, while UWB antenna senses the spectrum from 3 to 11 GHz. The antennas in [6]–[8] had sensing band from 2 to 11 GHz while reconfigurable antenna covered several frequencies between this sensing band. In [6] and [7], frequency agility was realized by rotational motion of antenna. In [8], antenna system based on photoconductive switch was proposed. In [9], reconfigurability was achieved by varying height and angle of ground plane. The sensing band was from 2 to 6 GHz while reconfigurable antenna had several operating bands between 2 to 6 GHz. In [10], a reconfigurable antenna with sensing capability was proposed. The antenna could reconfigure its frequency, gain patterns and polarization using PIN diodes. The antenna sensing band was from 3 to 12 GHz while reconfigurable bands were: 2.85, 2.5 and 4.7, 1.73, 1.88 and 5.23, 3.52 GHz. In [11], a reconfigurable and UWB antenna based on slot structure was presented. The proposed antenna had UWB mode for sensing and reconfigurable communication mode. The UWB band was from 2.8 to 11.4 GHz while reconfigurable communication band were: 3.2 to 4.5, 4.3 to 7.8 and 7.9 to 11.2 GHz. The antenna employed five PIN diodes to achieved reconfigurability. Majority of the antenna design presented in literature for CR applications use separate antennas for sensing and communication, and they have large size, complex structure and limited frequency tunability. Moreover, most of the reported antennas employed PIN diodes to obtain frequency agility and had distinct operating band. All these antennas had operating band over 2 GHz for the sensing and communication purposes.

Multiple-input multiple-output (MIMO) antennas are increasingly demanded in modern wireless communication system because of their capability to transmit data at higher rates and increase the channel capacity. Some MIMO reconfigurable antennas incorporated with UWB sensing antenna for CR applications were reported in literature [12]–[15]. In [12], a reconfigurable MIMO antenna can operate from 573 to 680 MHz and 834 to 1120 MHz while sensing band was between 0.72 to 3.44 GHz. In [13], MIMO reconfigurable filtennas based on monopole structure were presented for underlay and interweave system. The reconfigurable MIMO and sensing antenna had operating frequency band from 3 to 6 GHz. In [14], a planar inverted- F antenna (PIFA) based frequency agile MIMO antenna was presented. The reconfigurable antenna covered several bands from 0.75 to 3.45 GHz while the spectrum sensing antenna had operating band from 0.71 to 3.6 GHz. In [15], the frequency agile MIMO slot antenna had operating frequency band between 1.77 GHz to 2.51 GHz and UWB spectrum sensing antenna can operate from 0.75 GHz to 7.65 GHz. All these designs used separate antennas for sensing and communication. To the authors' knowledge, this is the first time that a single antenna has been utilized for frequency reconfiguration along with spectrum sensing capabilities as well as the same UWB antenna is used in MIMO configuration.

This paper presents a novel two-element antenna design with frequency reconfigurable MIMO mode and UWB spectrum sensing MIMO mode. The proposed antenna is based on modified triangular-shaped printed monopole antenna elements with combination of varactors and PIN diodes. The presented antenna can sense the frequency spectrum from 1 to 4.5 GHz in UWB MIMO mode using PIN diodes and then it provides frequency reconfigurability over wide range from 0.9 to 2.6 GHz using varactor diode tuning. The novelty of this antenna design is based on the fact that instead of two separate antennas, a single antenna can first sense the spectrum and then perform communication. The proposed antenna works in a sequential manner. Both modes work independently [16], and they have no effects on each other. Another novel feature of the presented antenna is that same UWB antenna has been utilized in MIMO configuration. The use of single antenna for spectrum sensing and reconfiguration reduces the total number of antennas needed and space requirements for CR system. The novelty of the presented design can also be accessed by compact single element size of 27×56 mm^2 while producing such wide frequency tuning range (i.e. from 0.9 GHz to 2.6 GHz) using only one varactor diode for each antenna element. To authors' knowledge, this type of compact antenna configuration with reconfigurable MIMO communication and UWB MIMO sensing capability has not been proposed so far for CR applications. The proposed antenna configuration and results are discussed in the next sections.

II. ANTENNA DESIGN

The design of the proposed frequency reconfigurable MIMO/UWB MIMO modified triangular-shaped monopole antenna system is shown in Fig. 1. The optimized dimensions of the proposed antenna are shown in Table 1. The antenna has total dimensions of 120×60 mm^2 and is printed on FR-4 substrate having a thickness of 1.5 mm, loss tangent of 0.02 and relative permittivity of 4.4. The bottom surface of antenna has ground (GND) plane and the GND plane size is 120×60 mm^2. Fig. 1 illustrates that the antenna structure comprises of two identical modified triangular-shaped printed monopole antenna elements (Ant1 and Ant2), six PIN diodes (D_1, D_2, D_3 D_5, D_6, and D_7) and two varactor diodes (D_4 and D_8) for frequency reconfiguration. Switching speed of the antenna depends on the switches/diode speed.

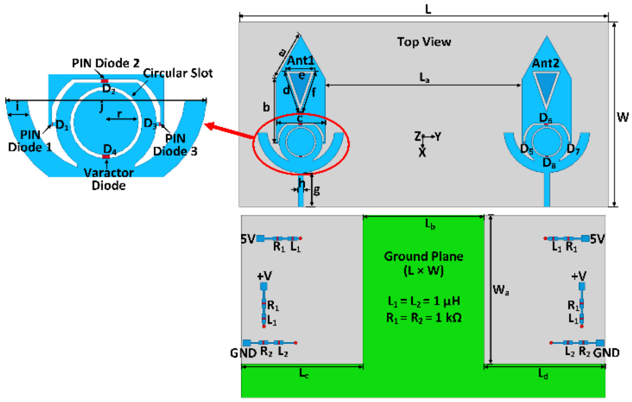

FIGURE 1. **Geometry of the proposed reconfigurable MIMO/UWB MIMO antenna.**

TABLE 1. **Detailed antenna dimensions.**

Parameter	L	W	L_a	L_b	L_c	L_d
Value (mm)	120	60	56	40	40	40
Parameter	W_a	a	b	c	d	e
Value (mm)	49	16.2	21.5	16.1	10.1	9.0
Parameter	f	g	h	i	j	r
Value (mm)	14.1	10.9	1.72	3.1	27	4.55

The PIN diodes used in the proposed antenna design were Infineon BAR63-03W and the varactor diode used were Infineon BBY6502V. These diodes provide fast switching speeds, high voltage handling capabilities and low power losses. According to the datasheet, switching time for PIN diode BAR63-03W is 75 ns. BBY6502V also has high tuning ratio at low supply voltage. Therefore, the proposed antenna has good performance with respect to switching speed as both these infineon products are suitable for this type of application.

The proposed CR front-end antenna can operate in UWB sensing mode and reconfigurable communication mode as described below.

A. UWB MIMO SENSING ANTENNA DESIGN

The UWB MIMO mode operates when all the PIN diodes (D_1, D_2, D_3 D_5, D_6, and D_7) are turned ON and two varactor diodes (D_4 and D_8) are reverse biased with 0 V. The PIN diodes are positioned in such a way that different switching conditions of PIN diodes makes the antenna dual-purpose. The PIN diode used were BAR63-03W. PIN diode was modeled as lumped RLC elements for ON/OFF condition based on forward biased and reverse biased lumped elements values provided in the datasheet. The different switching conditions of PIN diodes are achieved by providing 5 V DC supply in forward biased condition and 0 V in reverse biased condition. For UWB mode we require antenna with large metal area. The large metallization area required for UWB antenna is realized by turning ON all six PIN diodes. When PIN diodes D_1, D_2 and D_3 are switched ON for Ant 1, the upper portion of antenna is connected to lower portion and antenna works as UWB antenna.

B. RECONFIGURABLE MIMO ANTENNA DESIGN

To explain the frequency reconfigurable MIMO communication mode, geometry of a single element is described. The basic element used in the proposed design is a modified triangular-shaped printed monopole antenna with dimensions as shown in Table 1. The dimension of single antenna element is approximately 27 × 56 mm^2. The relative dimension in λ_g is $0.17\lambda_g \times 0.35\lambda_g$, which is considered compact as compared to other such designs available in literature. For frequency reconfigurable MIMO mode, varactor diode (D_4) is reverse biased with different voltage levels while the three PIN diodes (D_1, D_2, D_3) are turned OFF. To achieve frequency reconfigurability, a circular slot having a varactor diode (D_4) was incorporated into lower portion of antenna as shown in Fig. 1. The radius of the circular slot was r = 4.55 mm. The varactor diode used in the design were BBY6502V which has the working capacitance range 35–2.5 pF which corresponds to voltage range 0–5 V. Varactor diode was modeled as variable capacitor in simulation. Capacitive reactance of the slot was varied to obtain continuous frequency reconfigurable band with wide range tunability. This modified triangular-shaped printed monopole antenna element was radiating at 3.35 GHz. The reactive loading brought the resonant frequency band down from 3.35 GHz to sub 2 GHz bands. The reactive loading helped in reducing the antenna size by bringing the resonate band to lower frequency band.

Parametric analysis using HFSS were performed to understand the effect of antenna dimensions on its performance. The parametric study was conducted on one parameter at a time, while the rest of parameters were kept constant. The results of this study provided useful design guidelines and we obtained optimized dimensions for each parameter as shown in Table 1. Moreover, parametric study helped us to properly place varactors and PIN diodes in the design.

Fig. 1 also shows the biasing network used, which consists of resistors (R_1 and R_2) and RF choke (L_1 and L_2) in series. The variable voltage source was connected to varactor diode through series combination of resistors (R_1 and R_2) and RF choke (L_1 and L_2). Any AC from power supply was blocked by RF choke while the DC current from the antenna's radiating structure was blocked by varactor diode. The values for lumped elements were $R_1 = R_2 = 1$ kΩ and $L_1 = L_2 = 1\ \mu$ H.

III. RESULTS AND DISCUSSION

The prototype of antenna system was fabricated and measured to verify the design. Fig. 2 shows the fabricated prototype of the proposed frequency agile MIMO/UWB MIMO antenna fed by a 50 Ω microstrip feedline. The simulated results were obtained using ANSYS HFSS. Measurements for S-parameters were performed using vector network

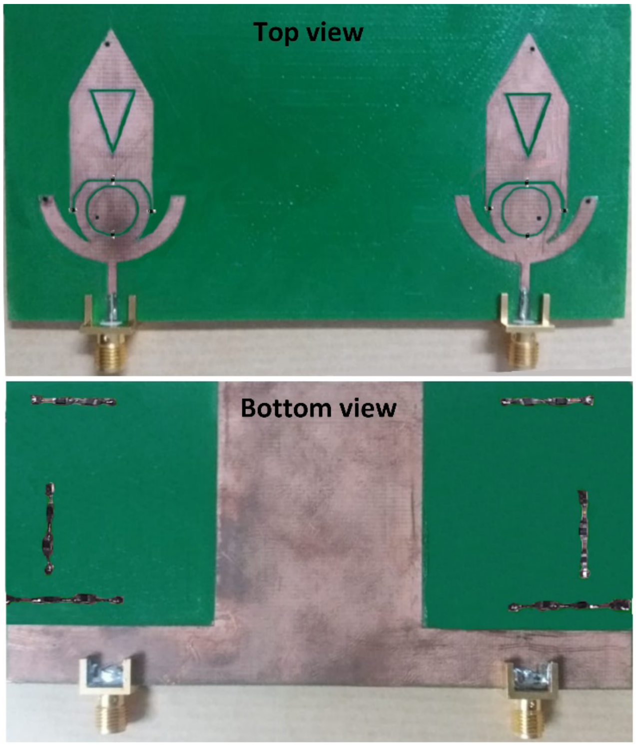

FIGURE 2. Fabricated antenna prototype.

analyzer while gain, efficiency, radiation patterns and ECC were measured using StarLab anechoic chamber.

A. UWB MIMO SPECTRUM SENSING MODE

The proposed antenna works in channel sensing mode when all PIN diodes (D_1, D_2, D_3 D_5, D_6, and D_7) are turned ON and two varactor diodes (D_4 and D_8) are reverse biased with 0 V. The simulated (black line) and measured (red line) reflection coefficients (S_{11}) of presented antenna in UWB sensing mode are compared in Fig. 3. The simulated and measured S_{11} in Fig. 3 shows that proposed antenna can cover the spectrum from 1 GHz to 4.5 GHz with minimum −10 dB bandwidth of 105 MHz in UWB mode. Overall simulated and measured results show good agreement. Structural tolerances during fabrication, which includes soldering tolerances, difference in substrate properties and diode effects are the possible causes of little discrepancy between simulated and measured results.

B. FREQUENCY RECONFIGURABLE MIMO MODE

Frequency reconfigurable MIMO mode is realized when varactor diodes D_4 and D_8 are reverse biased with different voltages from 0 to 5 V and all the PIN diodes are turned OFF. Fig. 4 presents the simulated and measured S_{11} results of proposed antenna in reconfigurable MIMO mode when varactor diode D_4 and D_8 are reverse biased. The simulated S_{11} in Fig. 4(a) shows that a resonant frequency continuously changes from 0.9 to 2.6 GHz when the capacitance of varactor diode is varied from 35 to 2.5 pF. The capacitance values used for simulated curves are C_1 = 35 pF, C_2 = 20 pF,

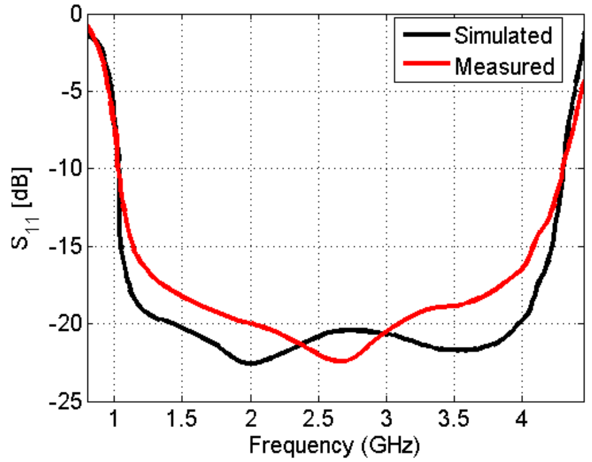

FIGURE 3. Simulated and measured reflection coefficient in UWB mode.

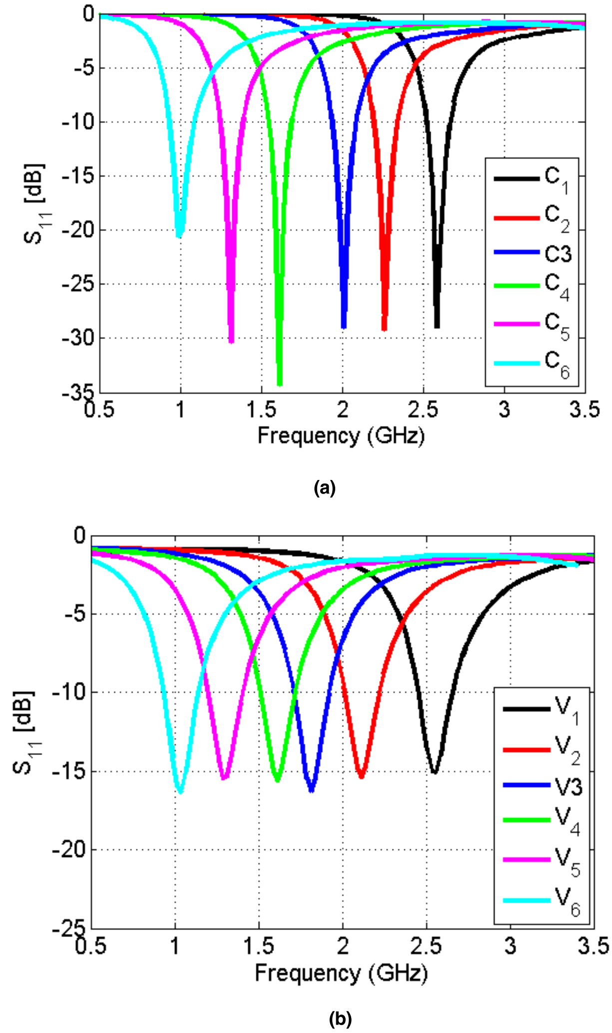

FIGURE 4. S_{11} results in reconfigurable communication mode (a) simulated S_{11} (b) measured S_{11}.

C_3 = 11 pF, C_4 = 4.5 pF, C_5 = 3.5 pF and C_6 = 2.5 pF. On the other hand, measured S_{11} result in Fig. 4(b) shows that a continuous frequency agility was obtained from 0.9 to 2.6 GHz by varying the varactor diode reverse bias voltage from 0 to 5 V. The measured curves shown are for voltage values of $V_1 = 0$ V, $V_2 = 1$ V, $V_3 = 2$ V, $V_4 = 3$ V, $V_5 = 4$ V and $V_6 = 5$ V. Hence, the proposed antenna achieves wide tunability from 0.9 GHz to 2.6 GHz in reconfigurable communication mode, covering popular wireless applications like GSM, UMTS, LTE, PCS, Bluetooth, WiFi and WiMAX. Moreover, very good impedance matching (below −10 dB) was achieved at each band. The −10 dB bandwidth for simulated and measured band were 105 MHz and 130 MHz respectively. A slight disagreement between simulated and measured results could be accounted to fabrication errors such as etching errors. Moreover, the soldering of varactor diodes and the placement of biasing circuitry was all done manually. As the proposed antenna has a symmetrical structure, S_{11} and S_{22} should be same. Hence, we only presented S_{11} results here.

Achieving good isolation between antenna elements is vital in MIMO antenna design for maintaining the benefit of improved MIMO capacity. For MIMO systems, an acceptable limit for port isolation is 10 dB. The simulated and measured isolation results between the two antenna elements are shown in Figs. 5(a) and 5(b). It is evident from the isolation curves that the isolation is less than −12.5 dB in the entire operating band. Therefore, the proposed antenna system shows good MIMO performance.

C. RADIATION PATTERNS AND EFFICIENCY

Fig. 6 compares the simulated and measured gain patterns in UWB mode at three frequencies at 1.1 GHz, 2.5 GHz and 4.5 GHz to get the complete illustration of the antenna behavior over the entire band. Fig. 7 shows the 2-D gain patterns of the presented antenna for reconfigurable communication mode at 1.65 GHz and 2.6 GHz for Ant 1 and Ant 2. These gain patterns are for *x-z* and *y-z* plane and measured by exciting one port and terminating other port to 50 Ω load. The proposed antenna system shows stable, nearly monopole like gain patterns across the entire tuning range. The simulated and measured gain as a function of frequency for the entire operating frequency range for the UWB and frequency reconfigurable communication mode is shown in Fig. 8. The proposed antenna shows acceptable gain for the MIMO operation for both the modes. The simulated and measured efficiencies, peak gain and the bandwidth of the proposed antenna in two modes are presented in Table 2. Overall simulated and measured values show good agreement. A little difference between simulation and measurements is attributed to fabrication errors and setup limitations. The measured maximum gain and efficiency were 3.98 dBi and 92.5% at 4.5 GHz respectively and minimum gain was 2.4 dBi with 88% efficiency at 1.5 GHz for UWB MIMO mode. In frequency reconfigurable MIMO mode, the minimum and maximum measured gain were 1.52 and 2.65 dBi respectively while measured efficiencies increased from 68 to 83% as frequency rises from 1.1 to 2.55 GHz. Hence, good

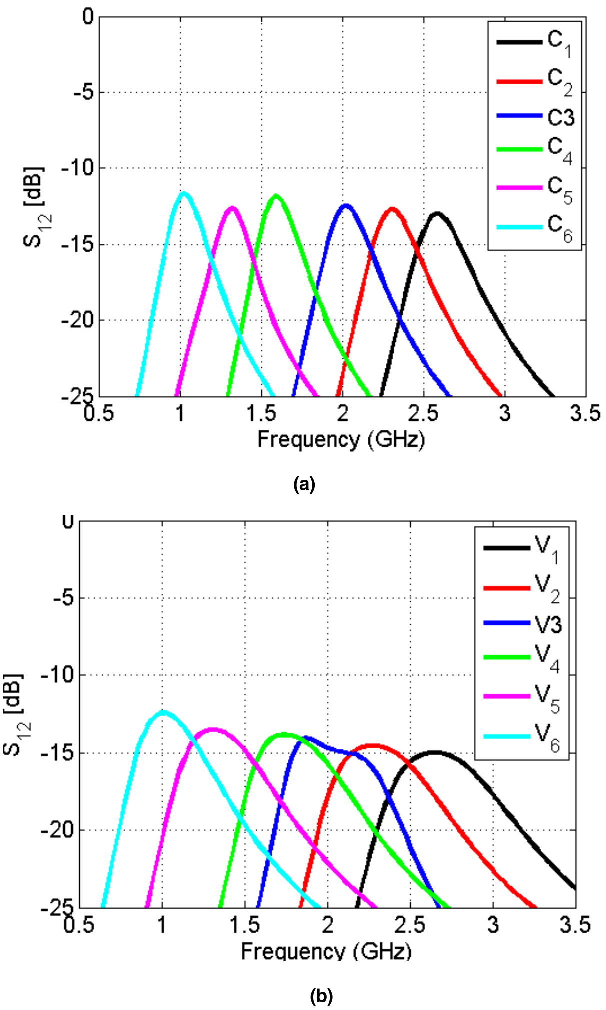

FIGURE 5. Isolation results in reconfigurable communication mode (a) simulated S_{12} (b) measured S_{12}.

gain and efficiency performance is obtained over the whole operating band for both modes.

Indoor anechoic chamber was used to measure the gain of the proposed antenna system. Indoor chambers are preferred to outdoor chambers because they offer several advantages i.e. controlled environment, capability in all weather, security, and reduced interference. The walls of the anechoic chamber are covered with RF absorbers to eliminate unwanted radiation interference with measurements. The gain measurements were started by illuminating the proposed antenna with a RF signal of correct frequency range from anechoic chamber ''source antennas''. The measurements involve setting up known calibrated reference antenna over radiated path in chamber, then zeroing (or normalizing) the path loss to 0 dB. The reference antenna chosen was horn antenna as it has wide frequency range (i.e. 300 MHz to 30 GHz) and we can measure gain over this entire operating range. The reference antenna was exchanged by proposed antenna and path loss/gain changes were measured relative to normalized reference path. By adding the reference antenna calibrated

TABLE 2. Simulated and measured antenna parameters.

Sim. center freq., GHz Sensing Band/Communication Band	1.5/ 1.0	2.0/ 1.35	2.5/ 1.62	3.5/ 2	4/ 2.25	4.5/ 2.6
Meas. center freq., GHz Sensing Band/Communication Band	1.5/ 1.1	2.0/ 1.3	2.5/ 1.65	3.5/ 1.75	4/ 2.15	4.5/ 2.55
Sim. B.W, MHz ($\|S_{11}\| \leq$ -10dB) Communication Band	105	107	110	115	125	135
Meas. B.W, MHz ($S_{11}\| \leq$ -10dB) Communication Band	130	137	141	145	153	165
Sim. effi., % Sensing Band/Communication Band	90/ 70	91.2/ 75	92/ 78	93/ 82	92/ 85	93/ 88
Meas. effi., % Sensing Band/Communication Band	88/ 68	89/ 70	91/ 75	90/ 80	91/ 81	92.5/ 83
Sim. Gain, dBi Sensing Band/Communication Band	2.5/ 1.8	2.52/ 1.9	2.7/ 2.5	3.2/ 2.9	3.6/ 2.5	3.7/ 2.45
Meas. Gain, dBi Sensing Band/Communication Band	2.4/ 1.52	2.43/ 1.75	2.65/ 2.44	3.05/ 2.65	3.42/ 2.4	3.98/ 2.1

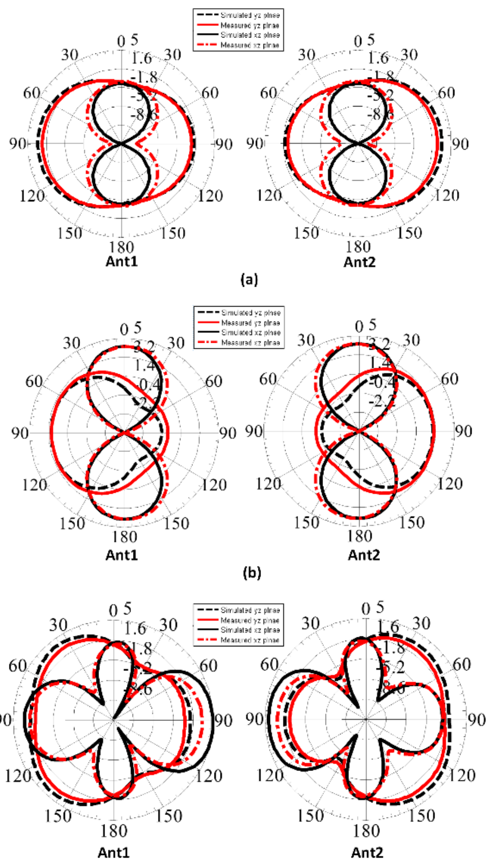

FIGURE 6. Simulated and measured radiation patterns of antenna elements in *x-z* and *y-z* planes for UWB MIMO mode at (a) 1.1 GHz (b) 2.5 GHz (c) 4.5 GHz.

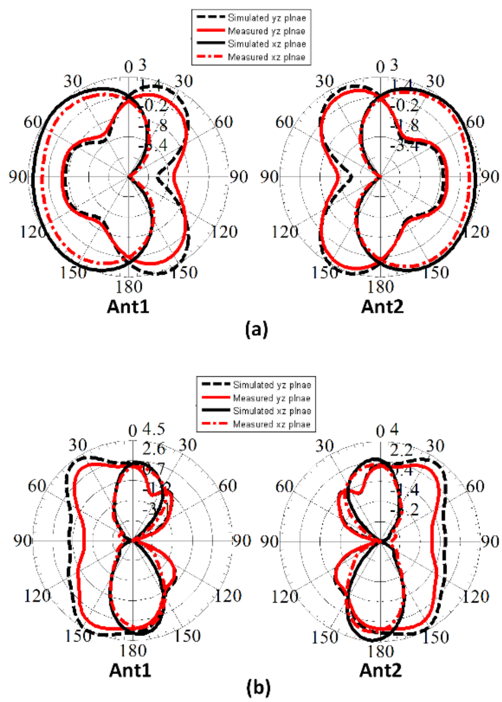

FIGURE 7. Simulated and measured radiation patterns of antenna elements in *x-z* and *y-z* planes for reconfigurable MIMO mode at (a) 1.65 GHz (b) 2.6 GHz.

gain to these measurements, we determined the antenna gain in dBi. As reconfigurable MIMO and UWB sensing modes are working independently, one antenna element was excited and other antenna element was terminated with 50-Ω load while performing measurements for efficiencies and radiation patterns of the proposed antenna system. Measurement setup for radiation pattern is shown in Fig. 9.

D. ECC

ECC is used to measure correlation between the antenna elements and it is an important performance metric for evaluating MIMO antennas. The MIMO antenna elements must satisfy the ECC < 0.5 criterion [17]. ECC can be calculated using radiation patterns [18]. A comparison between measured and simulated ECC between two antenna elements is shown in Table 3 for both UWB MIMO and frequency reconfigurable MIMO mode. It can be seen from Table 3 that worst ECC value was 0.162 at 4.5 GHz for UWB MIMO mode, while worst ECC value of 0.185 was observed for frequency reconfigurable MIMO mode at frequency of 1.65 GHz.

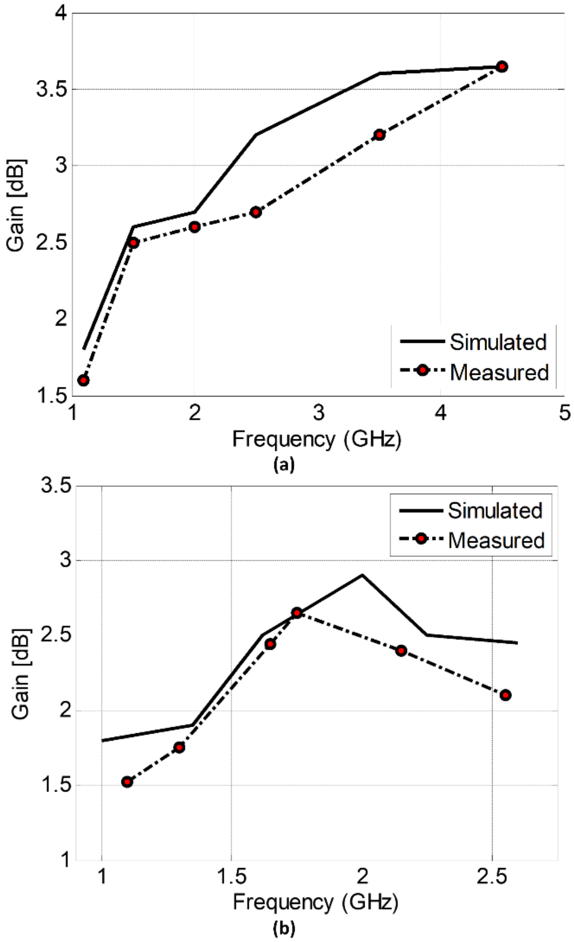

FIGURE 8. Simulated and measured gain of the proposed antenna in (a) UWB mode (b) frequency reconfigurable communication mode.

FIGURE 9. Measurement setup for radiation pattern.

The obtained ECC values are low which produce low signal correlation in multipath environment. Hence, the proposed antenna system displayed good MIMO performance for the complete operating band.

E. CURRENT DISTRIBUTION

Surface current distribution can be used to understand the coupling mechanism. Fig. 10 shows the current distribution for the proposed frequency reconfigurable MIMO/UWB MIMO antenna. Fig. 10(a) shows the current distribution for UWB mode at 3 GHz while Fig. 10(b) shows the current distribution for frequency reconfigurable communication mode at 2 GHz. In these figures, Ant1 was active while Ant2 was terminated with 50 Ω impedance. It is evident from the figure, that very low current distribution was observed around the lower edges for the frequency reconfigurable communication mode and the maximum energy was radiated in the UWB sensing mode as the current is taking longer path to travel so that it radiates at lower frequency bands.

TABLE 3. ECC values for the MIMO antenna elements.

UWB MIMO			Reconfigurable MIMO		
Freq. (GHz)	Sim. ECC_{12}	Meas. ECC_{12}	Freq. (GHz)	Sim. ECC_{12}	Meas. ECC_{12}
1.5	0.01	0.019	1.1	0.02	0.018
2	0.015	0.033	1.35	0.025	0.026
2.5	0.025	0.028	1.65	0.125	0.185
3.5	0.125	0.135	1.95	0.023	0.052
4	0.023	0.032	2.25	0.045	0.065
4.5	0.145	0.162	2.55	0.109	0.098

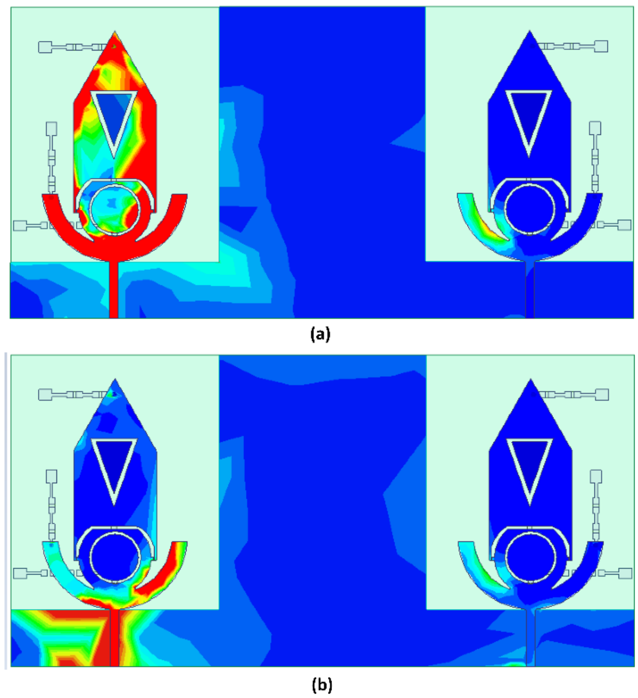

FIGURE 10. Surface current distribution for (a) UWB mode at 3 GHz (b) frequency reconfigurable communication mode at 2 GHz.

F. STATE-OF-THE-ART-COMPARISON

Table 4 compares the proposed antenna with recently published designs. It is apparent from the table that most of the antenna designs reported in literature use separate antennas for communication and sensing and had operating band over 2 GHz. The parameters compared in Table 4 were antenna size, achieved bands for communication and sensing,

TABLE 4. Comparison of proposed antenna with other existing antenna designs.

Ref.	Size (mm)	UWB Sensing Range (GHz)	Communication Bands (GHz)	Same Antenna for Sensing and Communication	UWB Antenna in MIMO Configuration
[3]	40 × 36	3.1–10.6	3.06–4.23, 4–6.37, 6.33–8.33, 8.7–9.92, 9.82–10.74	No	No
[4]	60 × 60	2–12	1.7, 2, 2.5, 2.94, 3.6, 4.5, 5, 5.48, 5.65	No	No
[5]	40 × 36	3–11	5–6	No	No
[6]	70 × 50	2–10	2.1–3, 3–3.4, 3.4–5.56, 5.4–6.2, 6.3–10	No	No
[7]	65.5 × 58	3.3–11	3.4–4.85, 5.3–9.15	No	No
[8]	50 × 45.5	3–11	3.2–4.3, 4.15–5.1, 4.8–5.7	No	No
[9]	70 × 70	2–6	2.4, 2.75, 4.2	No	No
[10]	85 × 85	3–12	1.73, 1.88, 2.5, 2.85, 3.52, 4.7, 5.23	Yes	No
[11]	21 × 9	2.8–11.4	3.2–4.5, 4.3–7.8, 7.9–11.2	Yes	No
[12]	120 × 65	0.72–3.44	0.57–0.68, 0.834–1.12	No	No
[13]	80 × 70	3–6	3.9, 4.215	No	No
[14]	120 × 65	0.71–3.6	1.095, 1.945, 3.05, 0.770, 1.66, 1, 1.508, 2.450, 3.350, 1.06, 1.760	No	No
[15]	120 × 60	0.75–7.65	1.77–2.51	No	No
Prop.	**120 × 60**	**1–4.5**	**0.9–2.6**	**Yes**	**Yes**

possible use of UWB antenna in MIMO configuration and whether same or different antennas were used for communication and sensing purposes. The comparison table shows that the proposed antenna displays a wide range continuous frequency tunability (0.9 to 2.6 GHz) for this frequency range and is the only design to use same UWB antenna in MIMO configuration as well.

IV. CONCLUSION

In this paper, a novel compact multi-mode frequency reconfigurable MIMO and UWB MIMO antenna is presented. The proposed two-port antenna is based on modified triangular-shaped printed monopole antenna design. The proposed antenna can work in sensing mode and reconfigurable communication mode without disturbing the characteristics of each other. The proposed antenna can cover the spectrum from 1 GHz to 4.5 GHz in the UWB mode using PIN diode switching while it provides wide frequency reconfigurable communication band from 0.9 to 2.6 GHz using varactor diode tuning. The single antenna element has compact size of 27×56 mm^2. The proposed antenna achieves good performance with respect to gain, efficiency, input impedance matching, isolation and ECC. The advantages of the presented design are its compact prototype, cost effective, low-profile structure and wide frequency reconfigurability using only one varactor diode per antenna element. To our knowledge, this is the first antenna design that has the capability of spectrum sensing as well as operating in MIMO configuration and then reconfiguring its operating frequency bands. Hence, the proposed design is a promising candidate for the present wireless communication antenna systems, particularly for handheld devices in CR applications.

REFERENCES

[1] J. Mitola, "Cognitive radio architecture evolution," *Proc. IEEE*, vol. 97, no. 4, pp. 626–641, Apr. 2009.

[2] C. G. Christodoulou, "Cognitive radio: The new frontier for antenna design?" *IEEE Antennas Propag. Soc. Feature Art*. to be published. [Online]. Available: www.ieeeaps.org

[3] A. Nella and A. S. Gandhi, "A five-port integrated UWB and narrowband antennas system design for CR applications," *IEEE Trans. Antennas Propag.*, vol. 66, no. 4, pp. 1669–1676, Apr. 2018.

[4] S. Sharma and C. C. Tripathi, "An integrated frequency reconfigurable antenna for cognitive radio application," *Radioengineering*, vol. 26, no. 3, pp. 746–754, 2017.

[5] E. Erfani, J. Nourinia, C. Ghobadi, M. Niroo-Jazi, and T. A. Denidni, "Design and implementation of an integrated UWB/reconfigurable-slot antenna for cognitive radio applications," *IEEE Antennas Wireless Propag. Lett.*, vol. 11, pp. 77–80, 2012.

[6] Y. Tawk, J. Costantine, K. Avery, and C. G. Christodoulou, "Implementation of a cognitive radio front-end using rotatable controlled reconfigurable antennas," *IEEE Trans. Antennas Propag.*, vol. 59, no. 5, pp. 1773–1778, May 2011.

[7] Y. Tawk and C. G. Christodoulou, "A new reconfigurable antenna design for cognitive radio," *IEEE Antennas Wireless Propag. Lett.*, vol. 8, pp. 1378–1381, 2009.

[8] Y. Tawk, J. Costantine, S. Hemmady, G. Balakrishnan, K. Avery, and C. G. Christodoulou, "Demonstration of a cognitive radio front end using an optically pumped reconfigurable antenna system (OPRAS)," *IEEE Trans. Antennas Propag.*, vol. 60, no. 2, pp. 1075–1083, Feb. 2012.

[9] J. Costantine, Y. Tawk, J. Woodland, N. Flaum, and C. G. Christodoulou, "Reconfigurable antenna system with a movable ground plane for cognitive radio," *IET Microw., Antennas Propag.*, vol. 8, no. 11, pp. 858–863, 2014.

[10] S. Sharma and C. C. Tripathi, "A novel reconfigurable antenna with separate sensing mechanism for CR system," *Prog. Electromagn. Res. C*, vol. 72, pp. 187–196, 2017.

[11] G. Srivastava, A. Mohan, and A. Chakrabarty, "Compact reconfigurable UWB slot antenna for cognitive radio applications," *IEEE Antennas Wireless Propag. Lett.*, vol. 16, pp. 1139–1142, 2017.

[12] R. Hussain and M. S. Sharawi, "A cognitive radio reconfigurable MIMO and sensing antenna system," *IEEE Antennas Wireless Propag. Lett.*, vol. 14, pp. 257–260, 2015.

[13] Y. Tawk, J. Costantine, and C. G. Christodoulou, "Reconfigurable filtennas and MIMO in cognitive radio applications," *IEEE Trans. Antennas Propag.*, vol. 62, no. 3, pp. 1074–1084, Mar. 2014.

[14] R. Hussain and M. S. Sharawi, "Integrated reconfigurable multiple-input–multiple-output antenna system with an ultra-wideband sensing antenna for cognitive radio platforms," *IET Microw. Antennas Propag.*, vol. 9, no. 9, pp. 940–947, 2015.

[15] R. Hussain, M. S. Sharawi, and A. Shamim, "An integrated four-element slot-based MIMO and a UWB sensing antenna system for CR platforms," *IEEE Trans. Antennas Propag.*, vol. 66, no. 2, pp. 978–983, Feb. 2018.

[16] R. Hussain and M. S. Sharawi, "Reconfigurable MIMO antennas for cognitive radios," in *Spectrum Access and Management for Cognitive Radio Networks*. Singapore: Springer, 2017, pp. 233–264.

[17] R. G. Vaughan and J. B. Andersen, "Antenna diversity in mobile communications," *IEEE Trans. Veh. Technol.*, vol. VT-36, no. 4, pp. 149–172, Nov. 1987.

[18] X. Zhao and S. Riaz, "A dual-band frequency reconfigurable MIMO patch-slot antenna based on reconfigurable microstrip feedline," *IEEE Access*, vol. 6, pp. 41450–41457, 2018.

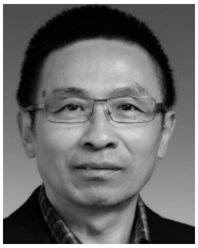

XIONGWEN ZHAO (SM'06) received the Ph.D. degree (Hons.) from the Helsinki University of Technology (TKK), Finland, in 2002.

From 1992 to 1998, he was with the Laboratory of Communications System Engineering, China Research Institute of Radiowave Propagation, where he was the Director and a Senior Engineer. From 1999 to 2004, he was with the Radio Laboratory, TKK, as a Senior Researcher and the Project Manager in the areas of MIMO channel modeling and measurements at 2, 5, and 60 GHz, as well as UWB. From 2004 to 2011, he was with Elektrobit Corporation, Espoo, Finland, as a Senior Specialist with EB Wireless Solutions. From 2004 to 2007, he worked in the European WINNER Project as a Senior Researcher in MIMO channel modeling for 4G radio systems. From 2006 to 2008, he also worked in the field of wireless network technologies, such as WiMAX and wireless mesh networks. From 2008 to 2009, he worked in mobile satellite communications for GMR-1 3G, DVB-SH RF link budget, and antenna performance evaluations. He is currently a Full Professor and the Chair of information and communications engineering with the North China Electric Power University, Beijing, China, and chairs several projects at the National Science Foundation of China, the Key Program of the Beijing Municipal Natural Science Foundation, the Beijing Municipal Science and Technology Commission, and the State Key Laboratories and Industries on radio channel and wireless power communications research. He is a Fellow of the Chinese Institute of Electronics (CIE). He was a recipient of the IEEE Vehicular Technology Society Neal Shepherd Memorial Best Propagation Paper Award, and the IEEE ISAPE Best Paper Award, in 2014 and 2018, respectively. He has served as a TPC member, Session Chair, and Keynote Speaker for numerous international and national conferences. He is a Reviewer of the IEEE transactions, journals, letters, and conferences.

SHARJEEL RIAZ received the B.S. degree in electrical engineering from the University of Engineering and Technology, Taxila, Pakistan, in 2006, and the M.Sc. degree in telecommunication engineering from the National University of Science and Technology, Pakistan, in 2009. He is currently pursuing the Ph.D. degree in electrical engineering with the North China Electric Power University, Beijing, China. He also worked as a Lecturer with the Electrical Engineering Department, Comsats Institute of Information Technology, Islamabad, Pakistan, where he was involved in various research projects and teaching. His research interests include design and analysis of MIMO antennas, reconfigurable antennas, and antennas for cognitive radio.

SUIYAN GENG received the M.Sc. (Tech.) and Ph.D. degrees from the Helsinki University of Technology (TKK), Espoo, Finland, in 2003 and 2011, respectively. From 1992 to 1998, she was a Research Engineer with the China Research Institute of Radiowave Propagation, Xinxiang, China. From 2001 to 2011, she was a Research Engineer with the Radio Laboratory (Department of Radio Science and Engineering, since 2008), TKK. She is currently an Associate Professor with the North China Electric Power University. She was a recipient of the IEEE Vehicular Technology Society (VTS) Neal Shepherd Memorial Best Propagation Paper Award, in 2014. Her research topics include millimeter-wave and ultra-wideband radio wave propagation and stochastic channel modeling for future-generation radio systems and technologies.